Doshi, M.M., C.S. Kulkarni, W.H. Ali, A. Gupta, P.F.J. Lermusiaux, P. Zhan, I. Hoteit, and O.M. Knio, 2019. Flowmaps and Coherent Sets for Characterizing Residence Times and Connectivity in Lagoons and Coral Reefs: The Case of the Red Sea. In: OCEANS '19 MTS/IEEE Seattle, 27-31 October 2019, doi:10.23919/OCEANS40490.2019.8962643

Flow Maps and Coherent Sets for Characterizing Residence Times and Connectivity in Lagoons and Coral Reefs: The Case of the Red Sea

Manan Doshi*, Chinmay S. Kulkarni*, Wael H. Ali*, Abhinav Gupta*, Pierre F. J. Lermusiaux*†,
Peng Zhan⋆, Ibrahim Hoteit⋆, Omar Knio⋆
*Department of Mechanical Engineering, Massachusetts Institute of Technology, Cambridge, MA
⋆King Abdullah University of Science and Technology
†Corresponding Author: pierrel@mit.edu

***Abstract*—To understand the dynamics and health of marine ecosystems such as lagoons and coral reefs as well as to understand the impact of human activities on these systems, it is imperative to predict the residence times of water masses and connectivity between ocean domains. In the present work, we consider the pristine lagoons and coral reefs of the Red Sea as an example of such sensitive ecosystems, with a large number of marine species, many of which are unique to the region. To study the residence times and connectivity patterns, we make use of recent advances in dynamic three-dimensional Lagrangian analyses using partial differential equations. Specifically, we extend and apply our novel efficient flow map composition scheme to predict the time needed for any particular water parcel to leave the domain of interest (*i.e.* a lagoon) as well as the time for any particular water parcel to enter that domain. These spatiotemporal residence time fields along with four-dimensional Lagrangian metrics such as finite time Lyapunov exponent (FTLE) fields provide a quantitative description of the Lagrangian pathways and connectivity patterns of lagoons in the Red Sea.**

***Index Terms*—Red Sea, Lagoons, Ocean modeling, Lagrangian field analysis, Residence time, Flow map composition, FTLE, Lagrangian coherent structures**

I. Introduction

Predicting the residence times and biophysical connectivity of ocean regions is extremely important to characterize the behaviors, dynamics, and health of marine ecosystems as well as to predict the effects of human activities in localized areas on the ecosystems connected to these areas. This is especially critical for the health and resiliency of marine lagoons and coral reefs. Considering the case of the Red Sea, its lagoons and coral reefs constitute an amazing undersea world home to 300 hard coral species and about 1,200 fish, of which 10 percent are local to the region. Its large number of lagoons along the coast (75 on the coast of Saudi Arabia) have large residence times that help coral growth due to the absence of erosion. However, the restricted exchange of water between these lagoons and the Red Sea is also responsible for pollution in the lagoons [19]. Characterizing the different connectivities in the region is thus very important. For example, [18] have showed that connectivity patterns can explain the gene diversity of the coral reefs found in the region.

To understand the connectivity patterns and study the exchange of water masses between various lagoons in the Red Sea, we resort to using Lagrangian field analyses. In the broadest sense, such analyses refer to studies performed using the Lagrangian viewpoint of fluid mechanics [14]. These field analyses provide a quantitative understanding of the transport characteristics of passive materials that flow with the fluid. They compute the attracting basins and repulsive surfaces, and accurately predict the flow patterns of such passive material through determining coherent and incoherent sets [4, 8, 13]. Extensive work has been done regarding Lagrangian transport in geophysical systems, and we refer the readers to [5, 6] for comprehensive reviews.

To address the challenges in lagoons and coral reefs, we utilize our recent advances in efficient four-dimensional (4D: time and space) Lagrangian field theory and methods [2, 3, 11, 12] for characterizing in a principled fashion the residence times and connectivity fields, showcasing the results for the Red Sea. Specifically, we study the connectivity patterns between the Eastern and Western coasts of the Red Sea Basin and the isolation of the southern part of the sea. By looking at how the structures of the flow evolve in presence of seasonal streams, we better understand the effects of these streams on connectivity patterns. Our approach is rooted in the fundamental Eulerian partial differential equations (PDEs) for the Lagrangian flowmap. With our novel numerical method of composition, we can solve these PDEs accurately and efficiently without compounding numerical errors [12]. As a result, instead of classic trajectory-based analyses, we provide accurate 4D field characterization of the Red Sea coherent water masses, residence time, and connectivity dynamic features. The long-term goal is to provide sustained 4D Lagrangian predictions, analyses, and characterizations of multiscale ocean transports, coherent structures, material sets, residence times, connectivity, and stirring and mixing processes in the Red Sea region.

978-0-578-57618-3

To represent the unsteady and multiscale nature of the ocean fields in the Red Sea region, we utilize the MIT general circulation model (MITgcm) [16] in 3D, including 8 major tidal components. The model is forced by hourly atmospheric fluxes, and a fine scale bathymetry field generated by assimilating several in situ observations is employed. The dynamical characteristics of the regional lagoon basins are mainly forced by tides at local scales, whereas the long term circulation inside the lagoons is driven by the general circulation outside the lagoon. Another motivation of the present work is to investigate these regional dynamics in the Lagrangian field sense and, in the future, collaborate with observational scientists to help design adaptive monitoring campaigns and plan principled optimal sampling strategies for characterizing the 4D residence times and connectivity fields in the lagoons and coral reefs.

The long-term objectives of the present collaborative Red Sea research are to: (i) Utilize our new Lagrangian field transport theory and methods to forecast, characterize and quantify ocean processes involved in the four-dimensional transports and transformation of water masses, and residence times in the Red Sea; (ii) Apply and expand our multi-resolution submesoscale-to-regional-scale ocean modeling, 2-way nesting, and uncertainty predictions, for real-time forecasting and process studies in the region; (iii) Help design field experiments and predict sampling strategies that maximize information on residence times, 4D pathways and dynamics in the region.

The manuscript is organized as follows. Section II overviews the state-of-the-art in Lagrangian analyses and our novel field PDE-based approach, with a specific focus on marine environments. Section III discusses the ocean modeling methodology and the regional oceanography of the Red Sea. We then showcase in Section IV selected results regarding the Lagrangian field dynamics of the Red Sea and its residence times, with an emphasis on specific lagoons. Finally, conclusions are provided in Section V.

II. Lagrangian Methods

A. Lagrangian Fields and Computation

We now briefly review the fundamentals of the Lagrangian viewpoint of material transport field analysis, and the associated recent advances. Typically, we denote any quantity that is being passively advected by the background fluid flow as a (passive) tracer, denoted henceforth by $\alpha(\mathbf{x}, t)$, where $\mathbf{x}$ is the (vectorial) position in the domain of interest Ω and t is the time, with $t \in [0, T]$. Examples of typical passive tracers include temperature, salinity, inertia-free particulate matters etc. We assume that the tracer quantity $\alpha(\mathbf{x}_0, t_0)$ that was at location $\mathbf{x}_0$ at time t_0 is passively transported with the underlying fluid parcel that was at location $\mathbf{x}_0$ at time t_0, and ends up at location $\mathbf{x}$ at time t. Thus, we have that:

$$\alpha(\mathbf{x}, t) = \alpha(\mathbf{x}_0, t_0) = \alpha_0(\mathbf{x}_0) \tag{1}$$

However, we know that the motion of the fluid parcel is governed by eq. 2.

$$\dot{\mathbf{x}}(t) = v(\mathbf{x}(t), t) \quad \text{given} \quad \mathbf{x}(t_0) = \mathbf{x}_0 \tag{2}$$

where $\mathbf{v}(\mathbf{x}, t)$ is the dynamic velocity field in the domain Ω. For the dynamical system given by eq. 2, the forward flow map between times t_0 and $t_1 (\geq t_0)$ is defined as:

$$\phi_{t_0}^{t}(\mathbf{x}_0) = \mathbf{x} \text{ where } \dot{\mathbf{x}}(t) = v(\mathbf{x}(t), t) \text{ with } \mathbf{x}(t_0) = \mathbf{x}_0 \tag{3}$$

That is, the forward flow map is simply the position of the fluid parcel at some later time (t) mapped onto its initial position (at time t_0). The inverse of the forward flow map, called the backward flow map is analogously given by eq. 4, where now the transport ODE 2 is solved in backward time with a specific terminal condition:

$$\phi_{t_0}^{t}(\mathbf{x}) = \mathbf{x}_0 \text{ where } \dot{\mathbf{x}}(t) = v(\mathbf{x}(t), t) \text{ with } \mathbf{x}(t) = \mathbf{x} \tag{4}$$

Substituting eq. 4 into eq. 1, we obtain eq. 5 that concisely states

$$\alpha(\mathbf{x}, t) = \alpha_0(\phi_{t_0}^{t}(\mathbf{x})) \ . \tag{5}$$

Eq. 5 suggests that computing a passive tracer transport ultimately amounts to accurately computing the flow maps of the underlying dynamical system and composing the said flow maps with the tracer initial condition.

The forward and backward flow map fields also provide a wealth of additional information. The singular values of the Jacobians of these maps, when scaled logarithmically are referred to as the 'finite time Lyapunov exponents' (FTLEs) [7, 17]. These forward and backward FTLE fields are commonly used to identify Lagrangian coherent structures (LCSs). The ridges of the forward FTLEs approximate the repelling manifolds: they tend to 'repel' water parcels. Two parcels that are close to each other at initial time but on different sides of the forward FTLE ridge will tend to advect farther away from each other than other parcels. The forward FTLEs thus act as material barriers to connectivity, and the forward FTLE ridges can be thought of as a skeleton to the connectivity pattern. On the other hand, the ridges of the backward FTLEs approximate the attracting manifolds: they tend to 'attract' water parcels. They thus increase the chances of connectivity among different water regions, ultimately by sub-mesoscale or turbulent mixing along the ridges in the backward FTLEs. Several other theories and metrics rooted in the flow map are used to determine attracting - repelling manifolds, coherent - incoherent material sets and other quantities of interest in fluid flows [4, 6, 8].

The typical trajectory-based approach to compute the flow maps is to appropriately solve eq. 2 in forward or backward time using certain time marching schemes for all possible initial conditions. However, the same can also be achieved by solving a single PDE whose characteristics are described by the said ODE. Specifically, one can obtain the backward flow map ϕ_t^0 by solving the PDE eq. 6 forward in time from time 0 to t, with the initial condition $\alpha_0(\mathbf{x}) = \mathbf{x}$:

$$\frac{\partial \alpha}{\partial t} + v \cdot \nabla \alpha = 0; \ \alpha_0(\mathbf{x}) = \mathbf{x} \text{ then } \alpha(\mathbf{x}, t) = \phi_t^0(\mathbf{x}) \ . \tag{6}$$

Similarly, the forward flow map ϕ_0^t is obtained by solving eq. 7 backward in time, with the terminal condition $\alpha_t(\mathbf{x}) = \mathbf{x}$:

$$\frac{\partial \alpha}{\partial t} + v \cdot \nabla \alpha = 0;\ \alpha_t(\mathbf{x}) = \mathbf{x} \text{ then } \alpha(\mathbf{x}, 0) = \phi_0^t(\mathbf{x})\ . \quad (7)$$

Once the flow map is computed, its associated quantities can be appropriately computed. Further, the flow map can be composed with the tracer initial condition to obtain the advected tracer field.

Finally, instead of computing the flow maps over the entire considered interval, one can also compute flow maps over smaller intervals and then compose them appropriately to obtain the flow maps over the larger time interval. Specifically:

$$\phi_{t_0}^{t_n} = \phi_{t_{n-1}}^{t_n} \circ \phi_{t_{n-2}}^{t_{n-1}} \circ \dots \phi_1^2 \circ \phi_0^1 \quad (8)$$

$$\phi_{t_n}^{t_0} = \phi_1^0 \circ \phi_2^1 \circ \dots \phi_{t_{n-1}}^{t_{n-2}} \circ \phi_{t_n}^{t_{n-1}} \quad (9)$$

We refer to this method are the 'method of flow map composition'. Composing such independent flow maps over smaller intervals presents the opportunity to parallelize the computation in the temporal direction, yielding a significant speedup. The individual flow maps are computed over a short interval and hence introduce minimal numerical errors. Further, the individual flow map computations are independent and hence the numerical errors are not compounded, which results in a much lower total error. Further details can be found in [12].

B. Residence Times Fields

Presently, we are primarily interested in efficiently computing the residence time fields in the domain of interest. These fields represent the time required for a water parcel that started at the considered position to leave the chosen domain of interest. An efficient approach to compute these fields is now developed.

Let Ω_D be the domain of interest in which we wish to compute the residence times. We initialize a hypothetical tracer field given by:

$$\alpha(\mathbf{x}) = \begin{cases} 1 & \forall \mathbf{x} \in \Omega_D \\ 0 & \text{otherwise} \end{cases}\ . \quad (10)$$

As stated earlier (eq. 5), the tracer concentration at a location $\mathbf{x}$ at some time t, *i.e.* $\alpha(\mathbf{x}, t)$ is computed using the initial tracer concentration ($\alpha_0(\mathbf{x})$) as:

$$\alpha(\mathbf{x}, t_i) = \alpha\left(\phi_{t_i}^0(\mathbf{x})\right)\ . \quad (11)$$

This equation can simply be inverted to obtain eq. 12.

$$\alpha_0(\mathbf{x}) = \alpha\left(\phi_0^{t_i}(\mathbf{x}), t_i\right)\ . \quad (12)$$

We can now use this initial concentration field to determine which water parcels (with their positions indexed at the initial time $t = 0$) will be inside or outside the domain of interest at $t = t_i$, specifically:

1) $\alpha_0(\mathbf{x}) = 0$ and $\mathbf{x} \in \Omega_D$ (inside-outside): Water parcel at $\mathbf{x}$ starts in the domain of interests and is outside the domain at time t_i.
2) $\alpha_0(\mathbf{x}) = 1$ and $\mathbf{x} \in \Omega_D$ (inside-inside): Water parcel at $\mathbf{x}$ starts in the domain of interests and stays in the domain at time t_i.
3) $\alpha_0(\mathbf{x}) = 0$ and $\mathbf{x} \notin \Omega_D$ (outside-outside): Water parcel at $\mathbf{x}$ starts from outside the domain and is outside the domain at time t_i.
4) $\alpha_0(\mathbf{x}) = 1$ and $\mathbf{x} \notin \Omega_D$ (outside-inside): Water parcel at $\mathbf{x}$ starts from outside the domain and is inside the domain at time t_i.

By computing these values at different times t_i we can construct the residence time fields based on when a water parcel exits the domain. Similar fields can be constructed to represent the intruding time fields as well as the other two cases described above.

III. Ocean Modeling and Regional Dynamics

A high-resolution MIT general circulation model (MITgcm) [16] was configured at KAUST for the coastal lagoon area offshore of Al Wajh region in the central Red Sea, extending from $36.35°E$ to $37.25°E$ and from $25.2°N$ to $26.4°N$ (Figure 1). The coastal model has a horizontal resolution of about 75 m and 50 vertical z-levels, the thickness of which gradually increases from 0.5 m at the surface to 180 m near the bottom. The model is nested within a regional 1-km model configured for the Red Sea with temperature, salinity, and horizontal velocity fields prescribed at the southern and western boundaries on a daily basis. Barotropic tidal currents are added through the amplitudes and phases extracted from the inverse barotropic tidal model TPXO 7.2 Indian Ocean (Red Sea) [REF], including eight major tidal components of semi-diurnal and diurnal frequencies (M2, S2, N2, K2, K1, O1, P1 and Q1). The model is forced by hourly surface wind, air temperature, specific humidity, precipitation, and downward shortwave and longwave radiation of a 3-km Weather Research Forecast (WRF) product [20] downscaled from ERAInterim products of the European Centre for Medium-Range Weather Forecasts (ECMWF) [1]. Various sources of data have been collected and merged to generate the fine-scale model bathymetry, including several in-situ cruise measurements that were conducted in the lagoon, the General Bathymetric Chart of the Oceans (GEBCO) [9] and satellite images from Google Earth.

At local scales in the Al Wajh region, tides constitute the major forces that determine the dynamical characteristics of lagoon-like basins; however, the long-term circulation inside the lagoons is primarily driven by larger-scale meteorological forces and the general circulation outside the lagoon. Northwesterly winds are dominant over the sea all over the year [15], while the wind regime from the land is more variable with smaller valleys cutting across the mountain ridges and lead to strong easterly jets [10]. The regional oceanic circulation commonly consists of a northward boundary current along the Saudi coast [21, 22], and frequent eddies that are more energetic during winter [23, 24, 25, 26]. Such eddy and boundary current events may affect the regional circulation outside the lagoon and potentially influence the flow inside.

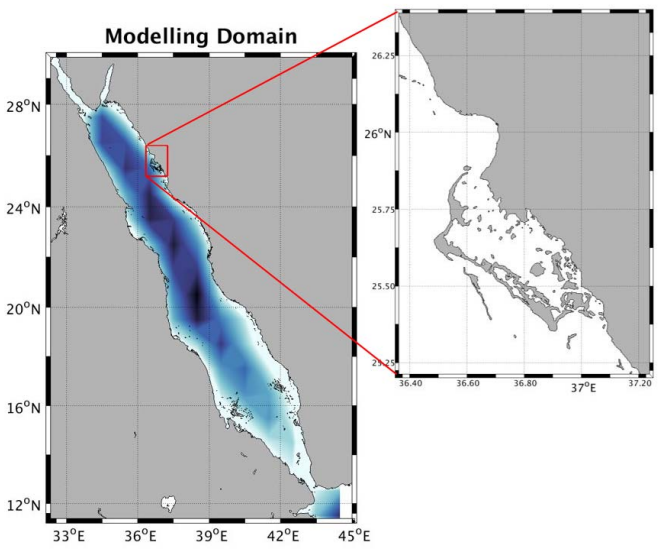

Fig. 1: Modelling Domains

IV. Lagrangian Dynamics and Residence Times Results

We now apply the above methodology to compute flow maps, FTLEs, and residence times in the Al Wajh region and overall Red Sea. We then showcase how the FTLE fields qualitatively depicts the skeleton of connectivity in these regions.

Figures 2 show the forward x and y flow maps at 0.25 m and Figure 3 the forward x, y and z flow maps 2.75 m, all plotted at the initial positions. That is, these maps collectively plot the final position (through x, y, and z coordinates, with z being positive downward) of a water parcel that started at a particular location at the start time. From the intensity in the gradients of the flow map, it can be seen that the amount of mixing in the Lagoon is much less than outside the Lagoon.

Figure 4 shows the vertical sections of the 3D x, y and z flow maps, with the Red Sea located to the left of the shown sections. The tall ridges in the repelling FTLE field signify very little mixing with the Red Sea. The z flow map shows upwelling at the eastern ridge of the Lagoon and downwelling on the western coast of the Lagoon. Hence, the regions of larger vertical transport within the Lagoon are located near its edges. Nutrient inputs can thus be expected to occur there as well.

The forward FTLE fields computed using the flow maps from Figure 2 are shown in Figure 5. We illustrate the forward FTLE for two different depths: 0.25 m (*i.e.* close to the surface) and 2.75 m from Nov. 3, 2017 to Nov. 10, 2017. As mentioned before, forward FTLEs tend to repel water parcels and thus act as barriers to connectivity. In Figures 5(a) and (b), we see a prominent FTLE ridge on the north side of the domain at both the considered depths. Further, we also highlight the existence of the ridges connecting the different small islands at the southwestern boundary of the lagoon. As the forward FTLEs form barriers to connectivity, these ridges together imply that during the 7-days considered, the water in the lagoon does not mix very well with the waters offshore at the southwestern boundary. This can be further confirmed by the FTLE fields over the entire red sea in Figure 6 (from Jan. 1, 2006 to Jan. 13, 2006), where we see prominent FTLE ridges between the Red Sea and the northeastern coastal regions. Moreover, there seems to be a significant amount of mixing of parts of the lagoon waters and the Red Sea on the northwest and southeast boundaries of the Al Wajh lagoon.

While the FTLE fields can indicate which waters of the lagoon are most likely (or not likely) to mix with the offshore Red Sea waters, they do not tell us directly where the mixing occurs spatially (*i.e.* whether the sea water enters the lagoon or whether the lagoon water enters the offshore sea). The aforementioned residence time fields can be utilized to perform this analysis.

To this end, Figure 7 shows residence time fields for water parcels inside the lagoon. Specifically, what is show is the amount of time it takes for a water parcel that started at the specific position to leave the lagoon. We observe that waters near the southeastern boundary exit the domain while those on the northwestern boundary remain inside the lagoon. We also see that the parcels that leave the domain are not uniformly spread out in the lagoon but form a distinct structure near the south eastern boundary. This egress happens mainly at the surface as the residence time fields at 2.75 m depth show significantly less water exiting the domain, see Figure 7(b). This is also verified by the stronger FTLE ridges at 2.75 m, see Figure 5(b), at the border of the lagoons implying lower horizontal mixing at depth.

Using our PDE-based Lagrangian methodology, we can also compute when waters from outside the Lagoon in the offshore Red Sea have entered the Lagoon. We refer to these fields as the "Entrance time" fields, as shown in Figure 8. We see that the outside waters enter the northwestern boundary of the Lagoon mainly at the surface. This is the portion of the offshore sea which we had predicted would mix with the waters in the Lagoon. We also note that the seawater parcels that enter the Lagoon form interesting filament structures, as seen in Figure 8.

Finally, we observe structures on the southwestern boundary of the Lagoon that enter the domain of interest. Since we predict that these waters in the Red Sea will not significantly mix with the Lagoon waters, we predict that most of these waters enter and then leave the lagoon domain during the period of interest, without significant mixing.

V. Conclusions

In this work, we studied the residence times and connectivity patterns of water masses in the Red Sea and Al Wajh Lagoon region. Such capabilities are of great use in characterizing the behavior, dynamics and health of the marine ecosystems native to the region.

To compute the residence times and connectivity patterns, we resort to recent advances in efficient four-dimensional

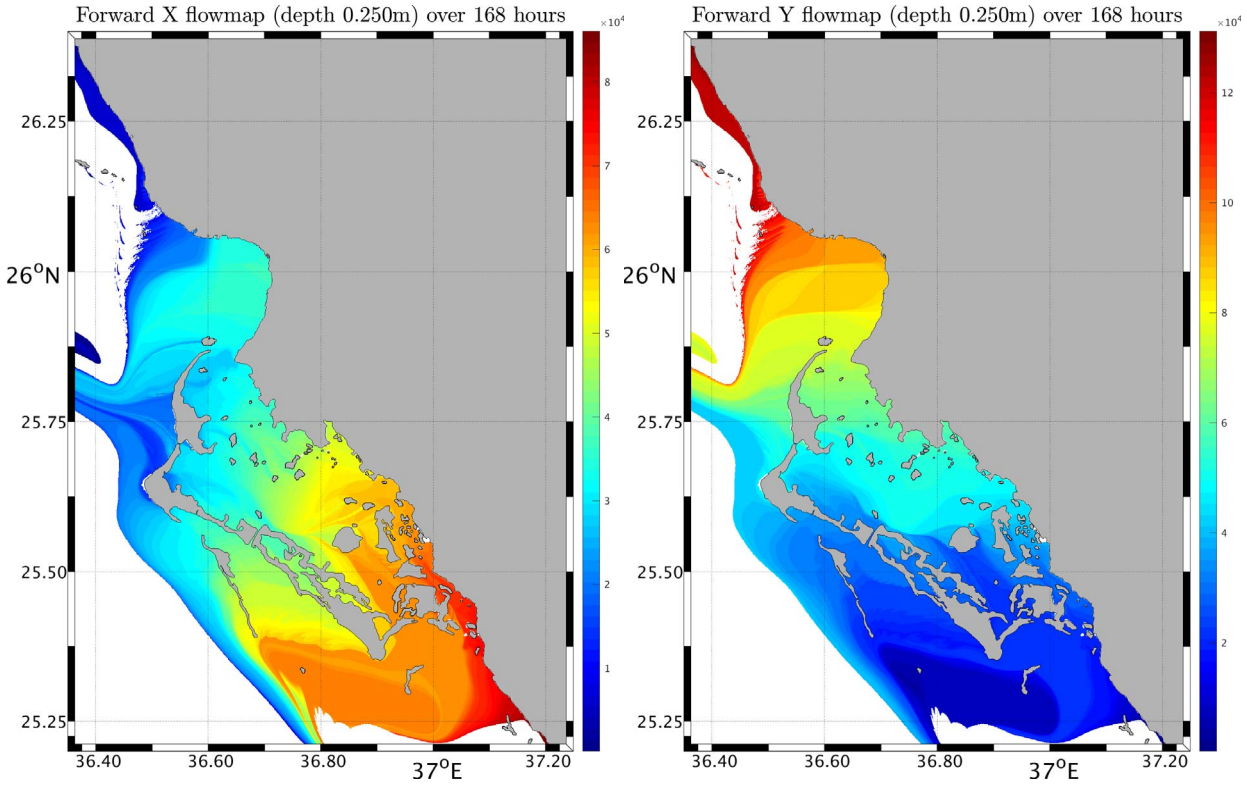

(a) x flow map (b) y flow map

Fig. 2: Forward flow maps (m) over the Al Wajh Lagoon modeling domain from 3 Nov, 2017 to 10 Nov, 2017 at 0.25 m.

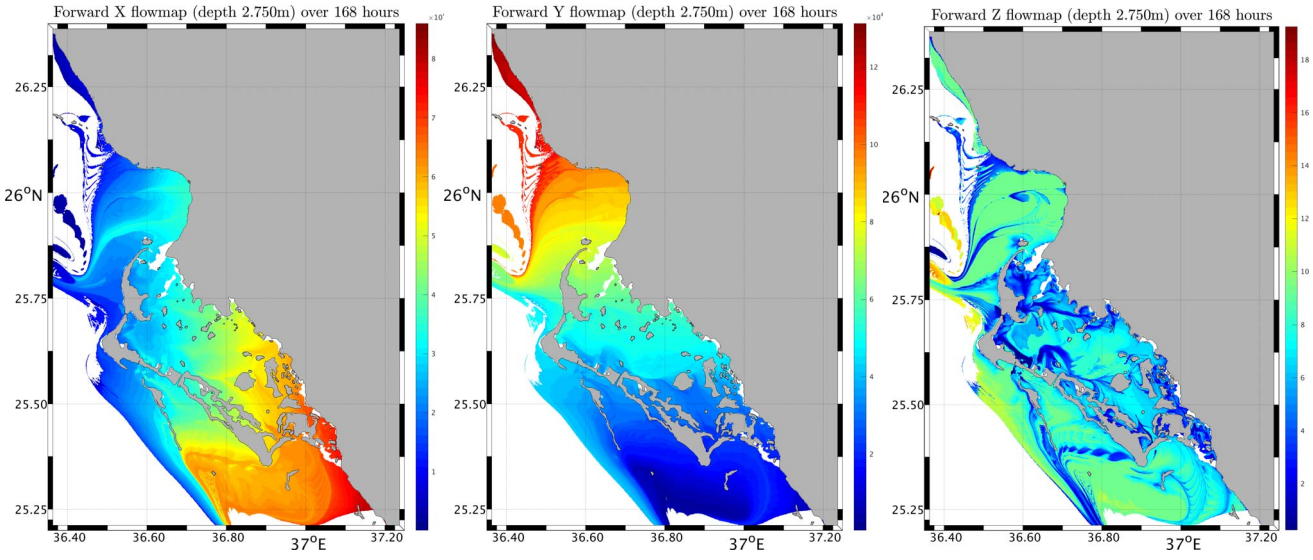

(a) x flow map (b) y flow map (c) z flow map

Fig. 3: Forward flow maps (m) over the Al Wajh Lagoon modeling domain from 3 Nov, 2017 to 10 Nov, 2017 at 2.75 m (z being positive downward).

(3D+time) Lagrangian analyses using partial differential equations. Specifically, we show how the method of composition can be efficiently used to compute the residence time fields, *i.e.* spatial fields that denote the amount of time a water parcel spends before exiting the domain of interest. With the same method, we also compute and describe the entrance time fields,

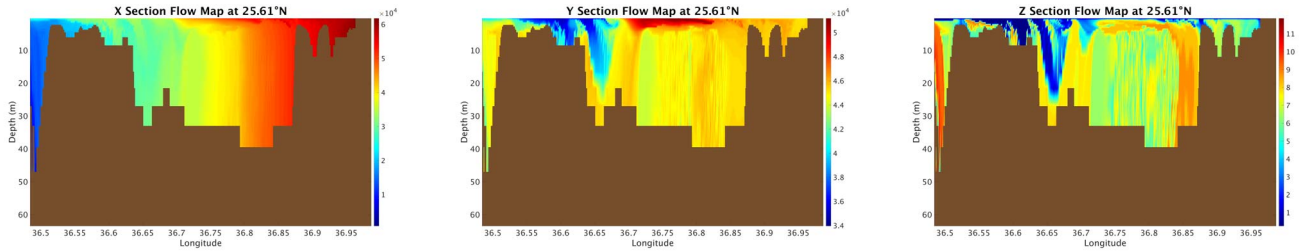

(a) x flow map (b) y flow map (c) z flow map

Fig. 4: Vertical section of forward flow maps over the Al Wajh Lagoon modeling domain from 3 Nov, 2017 to 10 Nov, 2017 at 25.61°N.

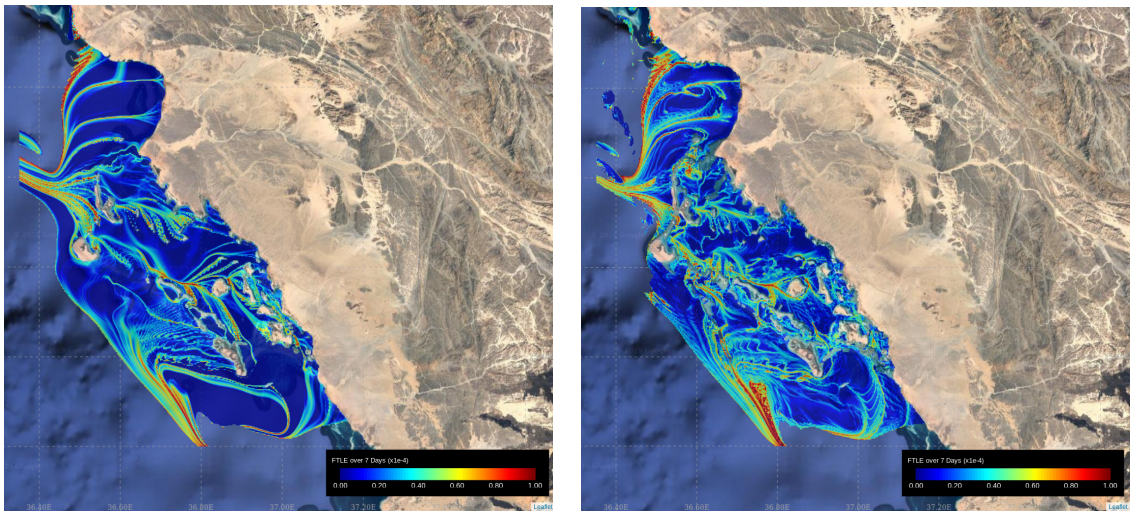

(a) forward FTLE at 0.25 m (b) forward FTLE at 2.75 m

Fig. 5: Forward FTLEs over the Al Wajh Lagoon modeling domain, from Nov. 3, 2017 to Nov. 10, 2017 at 0.25 m and 2.75 m, respectively.

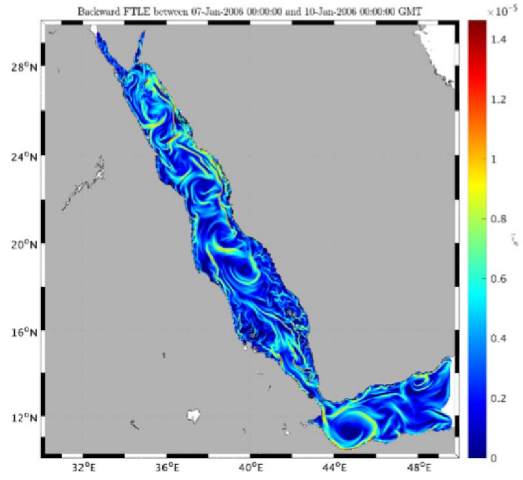

Fig. 6: Forward FTLEs over the entire Red Sea from Jan. 1, 2006 to Jan. 13, 2006.

i.e. spatial fields that denote the amount of time before water parcels offshore enter the domain of interest. We confirm that the ridges of the forward FTLE fields (approximating the repelling coherent structures) do indeed correspond to barriers to material flow, and we observe minimal water flux across these FTLE ridges in the simulations. That is, the residence time for most of the waters inside the Al Wajh Lagoon region is large, and a comparatively little amount of water mass leaves the Lagoon region. This indicates that even though the Lagoon waters are physically connected to the larger Red Sea offshore, they are only weakly connected in terms of material flow. This is especially important as the Lagoon ecosystem remains relatively protected from any major disturbances or events in the Red Sea. We believe that such in-depth scientific analyses of the biogeochemical ecosystems and their connectivities would go a long way in making informed policy decisions regarding their conservation.

ACKNOWLEDGMENTS

The study was supported by King Abdullah University of Science and Technology (KAUST) under the "Virtual Red

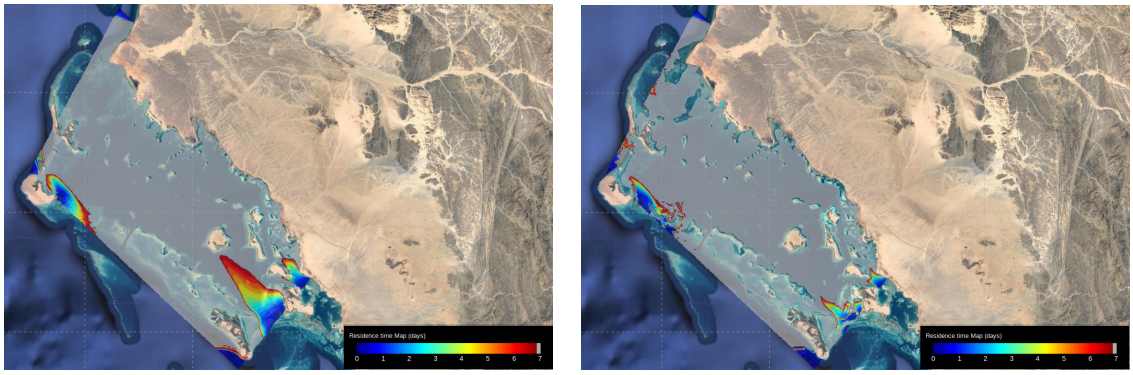

(a) Residence Time at 0.25 m (b) Residence Time at 2.75 m

Fig. 7: Residence time fields in the Al Wajh region, from Nov. 3, 2017 to Nov. 10, 2017 at 0.25 m and 2.75 m, respectively.

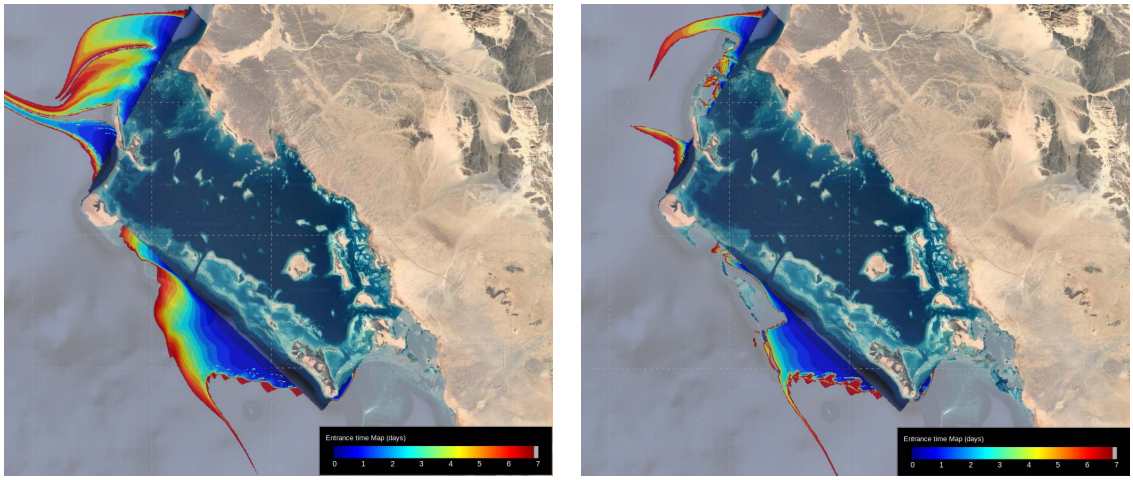

(a) Entrance Time at 0.25 m (b) Entrance Time at 2.75 m

Fig. 8: Entrance time fields in the Al Wajh region, from Nov. 3, 2017 to Nov. 10, 2017 at 0.25 m and 2.75 m, respectively.

Sea Initiative" award REP/1/32680101 and made use of the resources of the Supercomputing Laboratory and computer clusters at KAUST. The MSEAS group is also grateful to the Office of Naval Research (ONR) for support under grants N00014-14-1-0725 (Bays-DA), N00014-18-1-2781 (DRI-CALYPSO), and N00014-19-1-2693 (IN-BDA), and to the National Science Foundation for support under grant EAR-1520825 (NSF-ALPHA), all to the Massachusetts Institute of Technology.

References

[1] D. P. Dee, S. M. Uppala, A. J. Simmons, P. Berrisford, P. Poli, S. Kobayashi, U. Andrae, M. A. Balmaseda, G. Balsamo, P. Bauer, P. Bechtold, A. C.M. Beljaars, L. van de Berg, J. Bidlot, N. Bormann, C. Delsol, R. Dragani, M. Fuentes, A. J. Geer, L. Haimberger, S. B. Healy, H. Hersbach, E. V. Hólm, L. Isaksen, P. Kållberg, M. Köhler, M. Matricardi, A. P. Mcnally, B. M. Monge-Sanz, J. J. Morcrette, B. K. Park, C. Peubey, P. de Rosnay, C. Tavolato, J. N. Thépaut, and F. Vitart. The ERA-Interim reanalysis: Configuration and performance of the data assimilation system. *Quarterly Journal of the Royal Meteorological Society*, 2011.

[2] Florian Feppon and Pierre F. J. Lermusiaux. Dynamically orthogonal numerical schemes for efficient stochastic advection and Lagrangian transport. *SIAM Review*, 60(3):595–625, 2018.

[3] Florian Feppon and Pierre F. J. Lermusiaux. A geometric approach to dynamical model-order reduction. *SIAM Journal on Matrix Analysis and Applications*, 39(1):510–538, 2018.

[4] Gary Froyland, Simon Lloyd, and Naratip Santitissadeekorn. Coherent sets for nonautonomous dynamical systems. *Physica D: Nonlinear Phenomena*, 239(16):1527–1541, 2010.

[5] Annalisa Griffa, AD Kirwan Jr, Arthur J Mariano, Tamay Özgökmen, and H Thomas Rossby. *Lagrangian analysis and prediction of coastal and ocean dynamics*. Cambridge University Press, 2007.

[6] Alireza Hadjighasem, Mohammad Farazmand, Daniel Blazevski, Gary Froyland, and George Haller. A critical comparison of lagrangian methods for coherent structure detection. *Chaos: An Interdisciplinary Journal of Nonlinear Science*, 27(5):053104, 2017.

[7] George Haller. Lagrangian coherent structures. *Annual Review of Fluid Mechanics*, 47:137–162, 2015.

[8] George Haller, Alireza Hadjighasem, Mohammad Farazmand, and Florian Huhn. Defining coherent vortices objectively from the vorticity. *Journal of Fluid Mechanics*, 795:136–173, 2016.

[9] Iho Ioc. BODC, 2003. Centenary Edition of the GEBCO Digital Atlas, published on CD-ROM on behalf of the Inter-

governmental Oceanographic Commission and the International Hydrographic Organization as part of the General Bathymetric Chart of the Oceans. *British oceanographic data centre, Liverpool*, 2008.

[10] H S Jiang, T Farrar, R C Beardsley, R Chen, and C S Chen. Zonal surface wind jets across the Red Sea due to mountain gap forcing along both sides of the Red Sea. *Geophysical Research Letters*, 36, 2009.

[11] C. S. Kulkarni, P. J. Haley, Jr., P. F. J. Lermusiaux, A. Dutt, A. Gupta, C. Mirabito, D. N. Subramani, S. Jana, W. H. Ali, T. Peacock, C. M. Royo, A. Rzeznik, and R. Supekar. Real-time sediment plume modeling in the Southern California Bight. In *OCEANS Conference 2018*, Charleston, SC, October 2018. IEEE.

[12] Chinmay S. Kulkarni and Pierre F. J. Lermusiaux. Advection without compounding errors through flow map composition. *Journal of Computational Physics*, 398:108859, December 2019.

[13] Chinmay S. Kulkarni and Pierre F. J. Lermusiaux. Persistent rigid sets in realistic fluid flows using flow map composition. *Ocean Modelling*, 2019. In preparation.

[14] Cohen Ira M. Dowling David R. Kundu, Pijush K. *Fluid Mechanics*. Elsevier, 2012.

[15] Sabique Langodan, Luigi Cavaleri, Yesubabu Vishwanadhapalli, Angela Pomaro, Luciana Bertotti, and Ibrahim Hoteit. The climatology of the Red Seapart 1: the wind. *International Journal of Climatology*, 2017.

[16] John Marshall, Chris Hill, Lev Perelman, and Alistair Adcroft. Hydrostatic, quasi-hydrostatic, and nonhydrostatic ocean modeling. *Journal of Geophysical Research*, 102(C3):5733, 1997.

[17] Thomas Peacock and George Haller. Lagrangian coherent structures: The hidden skeleton of fluid flows. *Physics today*, 66(2):41–47, 2013.

[18] Dionysios E. Raitsos, Robert J. W. Brewin, Peng Zhan, Denis Dreano, Yaswant Pradhan, Gerrit B. Nanninga, and Ibrahim Hoteit. Sensing coral reef connectivity pathways from space. *Scientific Reports*, 7(1):9338, August 2017.

[19] Najeeb M. A. Rasul. Lagoon Sediments of the Eastern Red Sea: Distribution Processes, Pathways and Patterns. In Najeeb M.A. Rasul and Ian C.F. Stewart, editors, *The Red Sea: The Formation, Morphology, Oceanography and Environment of a Young Ocean Basin*, Springer Earth System Sciences, pages 281–316. Springer Berlin Heidelberg, Berlin, Heidelberg, 2015.

[20] Yesubabu Viswanadhapalli, Hari Prasad Dasari, Sabique Langodan, Venkata Srinivas Challa, and Ibrahim Hoteit. Climatic features of the Red Sea from a regional assimilative model. *International Journal of Climatology*, 2017.

[21] Fengchao Yao, Ibrahim Hoteit, Larry J Pratt, Amy S Bower, Armin Köhl, Ganesh Gopalakrishnan, and David Rivas. Seasonal overturning circulation in the Red Sea. 2: Winter circulation. *Journal of Geophysical Research: Oceans*, pages 2263–2289, 2014.

[22] Fengchao Yao, Ibrahim Hoteit, Larry J Pratt, Amy S Bower, Ping Zhai, Armin Köhl, and Ganesh Gopalakrishnan. Seasonal overturning circulation in the Red Sea: 1. Model validation and summer circulation. *Journal of Geophysical Research: Oceans*, pages 2238–2262, 2014.

[23] Peng Zhan, Ganesh Gopalakrishnan, Aneesh C Subramanian, Daquan Guo, and Ibrahim Hoteit. Sensitivity Studies of the Red Sea Eddies Using Adjoint Method. *Journal of Geophysical Research: Oceans*, 0(ja), 2018.

[24] Peng Zhan, George Krokos, Daquan Guo, and Ibrahim Hoteit. Three-Dimensional Signature of the Red Sea Eddies and Eddy-Induced Transport. *Geophysical Research Letters*, 46(4):2167–2177, feb 2019.

[25] Peng Zhan, Aneesh C Subramanian, Fengchao Yao, and Ibrahim Hoteit. Eddies in the Red Sea: A statistical and dynamical study. *Journal of Geophysical Research: Oceans*, 119(6):3909–3925, 2014.

[26] Peng Zhan, Aneesh C. Subramanian, Fengchao Yao, Aditya R. Kartadikaria, Daquan Guo, and Ibrahim Hoteit. The eddy kinetic energy budget in the Red Sea. *Journal of Geophysical Research: Oceans*, 121(7):4732–4747, 2016.